Molecular Physics, Vol. 103, Nos. 21–23, 10 November–10 December 2005, 3045–3054

Coarse-graining diblock copolymer solutions: a macromolecular version of the Widom–Rowlinson model

C. I. ADDISON†, J. P. HANSEN*†, V. KRAKOVIACK‡ and A. A. LOUIS†

†Department of Chemistry, University of Cambridge, Lensfield Road, CB2 1EW, Cambridge, UK
‡Laboratoire de Chimie, Ecole Normale Supérieure de Lyon, 69364 Lyon Cedex 07, France

(*Received 6 April 2005; in final form 24 May 2005*)

We propose a systematic coarse-grained representation of block copolymers, whereby each block is reduced to a single 'soft blob' and effective intra- as well as intermolecular interactions act between centres of mass of the blocks. The coarse-graining approach is applied to simple athermal lattice models of symmetric AB diblock copolymers, in particular to a Widom–Rowlinson-like model where blocks of the same species behave as ideal polymers (i.e. freely interpenetrate), while blocks of opposite species are mutually avoiding walks. This incompatibility drives microphase separation for copolymer solutions in the semi-dilute regime. An appropriate, consistent inversion procedure is used to extract effective inter- and intramolecular potentials from Monte Carlo results for the pair distribution functions of the block centres of mass in the infinite dilution limit.

1. Introduction

Recent years have witnessed considerable theoretical interest in statistical mechanics of multicomponent systems involving multiple length and time scales. To be tractable, statistical descriptions of such multi-scale systems must resort to controlled coarse-graining methods. One widely used coarse-graining strategy for complex fluids is to determine effective interactions between large ('dressed') particles (e.g. macromolecules or colloidal particles) by systematically tracing out the degrees of freedom of small particles (e.g. counter-ions or solvent molecules [1–3]). A particularly successful application has been to dilute and semi-dilute polymer solutions: effective interactions between polymer centres of mass (CM) are determined by taking appropriate averages over monomer conformations for fixed distances r between the *CM*s of interacting linear [4–7] or star polymers [1, 8]. In the case of linear polymers, to which the subsequent discussion will be restricted, the resulting *CM–CM* pair potential for polymers in good solvent, modelled by self-avoiding walks (SAW) on a cubic lattice, is very soft, repulsive and finite at all separations r, with a range of the order of the radius of gyration R_g of the polymer coils. The general shape is reasonably well represented by a Gaussian of amplitude on the order of k_BT, reflecting the essentially entropic nature of the effective interaction. While the overall form of the effective pair potential is not very sensitive to polymer concentration under good solvent or high temperature conditions, it turns out to be very sensitive to concentration and temperature when the latter is lowered toward the θ solvent regime [6, 9].

Replacing a full monomer level representation of polymer coils by a 'soft particle' description based solely on effective pair potentials between *CM*s represents a considerable reduction in the number of degrees of freedom, and hence leads to a concomitant reduction in computational effort in simulations of large-scale phenomena involving many polymers. Moreover, use of spherically symmetric effective pair potentials allows a direct exploitation of the theoretical arsenal developed over the years for the study of the bulk [10] and interfacial [11] properties of simple fluids. Last, but not least, inspection of the effective pair potentials leads to new insights into the phase behaviour [2] and stability [6] of macromolecular solutions.

In this paper we extend the above coarse-graining strategy to the case of solutions of block copolymers and more specifically to symmetric diblock copolymers made up of two strands A and B of equal length. AB copolymers will be reduced to 'soft diatomics', with inter- and intra-molecular interactions between sites

*Corresponding author. Email: jph32@cus.cam.ac.uk

Molecular Physics
ISSN 0026–8976 print/ISSN 1362–3028 online
http://www.tandf.co.uk/journals
DOI: 10.1080/00268970500186086

associated with the *CM*s of A and B strands. The nature of A–A, A–B and B–B effective pair interactions depends on solvent conditions. Most of the results presented in this paper will be based on a simplified model inspired by the celebrated Widom–Rowlinson (WR) model for fluid–fluid phase separation [12]. In the macromolecular extension of the WR model, A and B strands are mutually avoiding (i.e. monomers of opposite species cannot overlap) while A and B strands will separately behave like ideal (Gaussian) chains, i.e. they will freely interpenetrate same species strands on different copolymers.

2. Model and coarse-graining strategy

We consider lattice models of polymers, where monomers occupy the sites of a periodically repeated simple cubic lattice of size Λ^3; the bond vectors connecting successive monomers point along the x, y or z directions only. Each polymer comprises $\mathcal{M}$ monomers and hence $L = \mathcal{M} - 1$ bonds (or segments), such that the length of the polymer is Lb, if b is the segment length. A diblock copolymer AB is made up of two strands comprising M_A and M_B monomers respectively, with the M_Ath monomer of strand A connected to the first monomer of strand B. The total length is $(L_A + L_B + 1)b = (M_A + M_B - 1)b$. Restriction will be made here to symmetric copolymers, such that $M_A = M_B = M$ and $L_A = L_B = L$. We will consider N such copolymers on a Λ^3 lattice, such that the A and B monomer concentrations are $c_A = c_B = MN/\Lambda^3$ and the overall monomer concentration is $c = c_A + c_B$. Individual copolymer chains are characterized by three radii of gyration R_{gA}, R_{gB} and R_g, defined as usual by

$$R_{gA}^2 = \frac{1}{M_A}\sum_{i=1}^{M_A}\langle(\mathbf{r}_i^A - \mathbf{R}_A)^2\rangle, \tag{1}$$

where $\mathbf{r}_i^A$ is the position of the ith monomer of species A on the lattice, while $\mathbf{R}_A = \sum_{i=1}^{M_A}\mathbf{r}_i^A/M_A$ is the position of the centre of mass (*CM*) of strand A. The statistical average $\langle\cdot\rangle$ is taken over properly weighed chain conformations. Similar definitions hold for R_{gB} and for the overall radius of gyration R_g; the overall *CM* is $\mathbf{R} = (\mathbf{R}_A + \mathbf{R}_B)/2$. Another important length is the root mean square distance between the *CM*s of the two strands of a copolymer:

$$R_{AB} = \left[\langle|\mathbf{R}_A - \mathbf{R}_B|^2\rangle\right]^{1/2}. \tag{2}$$

An elementary calculation shows that:

$$R_g^2 = \frac{1}{2}R_{gA}^2 + \frac{1}{2}R_{gB}^2 + \frac{1}{4}R_{AB}^2. \tag{3}$$

The A–A, A–B and B–B interactions between non-adjacent monomers of the same or opposite species determine the structure and phase behaviour of individual copolymers and of many-copolymer systems. A number of models have been examined in the polymer literature: the more interesting are those which account for some degree of incompatibility between A and B monomers, which leads to microphase separation [13, 14]. In this paper we focus on the simplest, athermal models combining ideal (or random walk, with backward overlapping steps allowed) strands (I) and excluded volume (self or mutually avoiding walks) strands (S). The eight possible combinations of monomer interactions will be labelled by three indices JKL, with each index either I or S. The first index refers to the interaction between A monomers (on the same or different polymers), the second index refers to the A–B cross-interaction, while the last index refers to the B–B interaction. Of the eight possible combinations, two (III and SSS) reduce to homopolymers of molecular weight $2M$, while IIS and SII as well as ISS and SSI are degenerate for the symmetric ($M_A = M_B$) copolymers considered here, leaving four distinct, non-trivial copolymer models, namely IIS, ISI, ISS and SIS. Among these, the ISI model may be regarded as the macromolecular equivalent of the WR model [12]. The macroscopic phase separation occurring in the latter is prevented here because A and B strands are tethered, but microphase separation into a lamellar structure may be expected. Most of the subsequent discussion is hence devoted to the ISI model.

Physically, self-avoiding walks and random walks (ideal polymers) reflect solvent conditions. The former model corresponds to good solvent conditions associated with swollen chains, while random walk polymers are generally considered as approximating θ-solvent conditions, at least for low polymer concentrations [15]. Thus in the ISI model, A and B strands behave individually as if they were in a θ-solvent, where monomer excluded volume effects are compensated by nearest-neighbour, solvent-induced attraction, while A–B interactions are purely of excluded volume nature (mutually avoiding walks). A more general model than those considered here contains both excluded volume interactions (single occupancy constraint) and nearest neighbour interactions $\epsilon_{\alpha\beta}$ (α, β =A or B), thus introducing an explicit temperature dependence. This standard model has been extensively studied both in

the low concentration (single copolymer) limit [16] and in the melt [14]. The present investigation covers special cases of the generic model for finite copolymer concentrations, in the dilute and semi-dilute regimes. The key characteristic of these models, and in particular of the ISI model, is their extreme non-additivity, as in the WR model.

The range of concentrations which will be considered is best characterized by the ratio of the copolymer density, $\rho = N/(\Lambda b)^3$ over the overlap density $\rho^* = 3/(4\pi {R_g}^3)$, where R_g is the radius of gyration at zero density. Dilute solutions correspond to $\rho/\rho^* \ll 1$, while the semi-dilute regime is for $\rho/\rho^* \geq 1$.

The coarse-graining strategy which we shall pursue generalizes that developed earlier for linear homopolymers [4–6]. An AB block copolymer will be represented by two spherical 'blobs' centred on the *CM*s $\mathbf{R}_A$ and $\mathbf{R}_B$, and tethered by an anharmonic entropic spring deriving from an intramolecular potential $\phi_{AB}(r)$, where $r = |\mathbf{R}_A - \mathbf{R}_B|$. The A and B blobs on different copolymers will interact via effective pair potentials $v_{AA}(r)$, $v_{AB}(r)$ and $v_{BB}(r)$ acting between the *CM*s. As in the earlier work on homopolymers, these four effective potentials are determined by an inversion procedure based on the *CM–CM* pair distribution functions $s_{AB}(r)$ (intramolecular) and $g_{AA}(r)$, $g_{AB}(r)$ and $g_{BB}(r)$ (intermolecular). The latter are determined by Monte Carlo (MC) simulations of the initial, monomer-level model.

In this paper these pair distribution functions and resulting effective pair potentials will be determined only in the low concentration limit, by simulating copolymer pairs. While the inversion procedure is trivial in that limit in the case of homopolymers (represented by single blobs), it turns out to be much more involved in the copolymer case, since four effective blobs are involved, as will be discussed in more detail in section 4.

3. Monte Carlo results

With the above coarse-graining objective in mind, we have carried out extensive MC simulations of symmetric AB diblock copolymers on a cubic lattice. Most simulations were for the ISI model, but some preliminary results have also been obtained for the IIS, ISS and SIS models; test runs were carried out for the SSS model to compare with previous results of the equivalent SAW homopolymers.

MC runs were carried out on periodic lattices of size at least $\Lambda = 100$. The numbers of copolymers were adjusted to achieve any given polymer density ρ/ρ^*; thus N was taken to be 1 to determine infinite dilution, single polymer properties, $N = 2$ if effective pair interactions were to be determined in that limit, while for $\rho/\rho^* \geq 1$, N varied between a few hundred and over a thousand. The number of monomers $2M$ in each strand of a copolymer was varied between 60 and 1000. Configuration space was sampled by using pivot and translation moves [17, 18], polymers were subjected to between 5×10^5 and 10^8 MC moves, depending on the total number of polymers in the system.

Table 1. Radii of gyration R_g, mean intramolecular distance R_{AB} and second virial coefficient B_2 in units of R_g ($2M = 500$ only) for ideal/SAW systems.

Type	R_g	R_{gA}	R_{gB}	R_{AB}	B_2
$2M = 320$					
ISI	8.19	5.27	5.28	14.11	
IIS	9.99	5.16	8.53	12.47	
ISS	10.85	5.27	8.69	16.08	
SIS	12.13	8.55	8.50	17.11	
SSS	12.96	8.70	8.64	19.14	
$2M = 500$					
ISI	10.228	6.588	6.586	18.23	4.84
IIS	12.902	6.455	11.146	15.60	3.76
ISS	13.872	6.560	11.279	20.66	5.71
SIS	15.798	11.148	11.146	22.34	3.87
SSS	16.831	11.273	11.271	24.96	5.70
$2M = 2000$					
ISI	20.47	13.20	13.18	40.32	
IIS	28.94	13.13	25.54	31.28	
ISS	30.33	13.13	25.59	45.23	
SIS	35.95	25.38	25.36	50.44	
SSS	38.39	26.06	26.04	56.23	

Results for the three radii of gyration and the mean *CM–CM* distance R_{AB} are collected in table 1, for the four copolymer models as well as for the SSS model, which serves as a check against the well-documented SAW homopolymer model, for which $R_g \simeq 0.44L^{\nu}$ with $\nu \simeq 0.587$ in the scaling limit [19]. The trends in the various quantities in table 1 for the various models agree qualitatively with expectation. The internal *CM–CM* pair distribution function s_{AB} and the resulting 'entropic spring' potential, i.e. the effective bonding potential between the *CM*s of the A and B strands of a single copolymer

$$\phi_{AB}(r) = -k_B T \ln s_{AB}(r), \tag{4}$$

are plotted in figure 1. While the distribution functions $s_{AB}(r)$ for the IIS and SIS models peak at the origin, as one might expect since both strands can freely interpenetrate in both cases, the $s_{AB}(r)$ have peaks at $r > R_{gm}$, where $R_{gm} = (R_{gA} + R_{gB})/2$, in the ISI, ISS and SSS models, because of the single occupancy

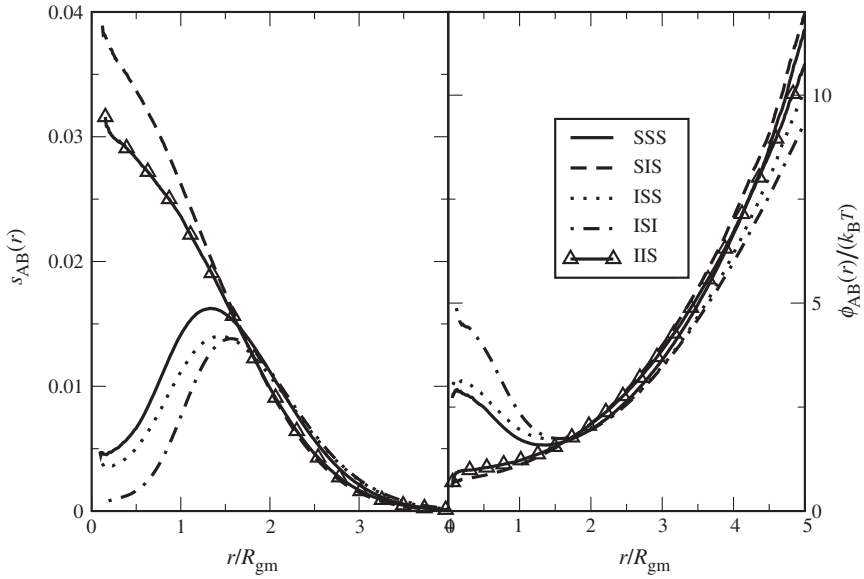

Figure 1. Left: zero density limit of the intramolecular *CM*-pair distribution function $s_{AB}(r)$ for different models, versus r/R_{gm}, where $R_{gm} = (R_{gA} + R_{gB})/2$ is the mean radius of gyration of the A and B strands. Right: the corresponding intramolecular pair potentials $\phi_{AB}(r)$, in units of k_BT, defined in equation (4).

constraint on monomers of opposite species in all three cases. Hence these three copolymer models behave like macromolecular diatomics, i.e. they are, on average, elongated, as confirmed by inspection of the eigenvalues of their tensor of inertia (not shown here). The corresponding intramolecular potentials ϕ_{AB} exhibit a maximum at full overlap ($r = 0$) and a minimum for $r \simeq 1.5R_{gm}$. Beyond that minimum, all potentials increase rapidly, illustrating the 'entropic spring' character of the effective interaction between the *CM*s of the two strands. Because the two strands are tethered, ϕ_{AB} must diverge when $r \to L \times b$, corresponding to the highly improbably fully stretched conformation of the AB copolymers. Note that relative to the $r = 0$ value, the potential minimum is considerably deeper for the ISI model, compared with the ISS and SSS models. In other words elongated conformations have higher probability for the ISI model. This is because the two ideal strands in the latter model are more compact than self-avoiding strands, as reflected in their shorter radii of gyration. The potential barrier to interpenetration of mutually avoiding strands is thus larger when the strands are individually ideal, since the probability of the forbidden overlap of monomers of opposite species is larger. The results discussed so far are for isolated copolymers. We henceforth restrict all further considerations of many polymer systems to the ISI model.

We first investigate the influence of polymer concentration on the intramolecular *CM* distribution function $s_{AB}(r)$. Figure 2 shows the MC data for the ISI model at four different concentrations, as well as the corresponding R_{AB}, which is related to the properly normalized $s_{AB}(r)$ by:

$$R_{AB}^2 = 4\pi \int_0^{Lb} s_{AB}(r) r^4 \, dr. \tag{5}$$

$s_{AB}(r)$ is seen to be rather insensitive to concentration in the dilute regime as one might intuitively expect and R_{AB} contracts slightly as ρ/ρ^* increases before expanding at higher densities where microphase separation sets in. In terms of the coarse-grained diatomic analogy, this means that the two-blob 'molecule' hardly contracts upon compression and that this coarse-grained entity remains a valid concept in the semi-dilute regime. Note however that the 'entropic spring' potential ϕ_{AB} is no longer given by equation (4) at finite concentration, because the problem ceases to be a purely two-body one. A more complex inversion procedure is required, to which we return in section 4.

In order to gain more insight into the physical significance of the ISI model, we have determined the osmotic equation of state of the model in the dilute and semi-dilute regimes. The equation of state can be efficiently and accurately determined in a single MC run, by subjecting the copolymers to a gravitational field until sedimentation equilibrium is reached, determining the resulting inhomogeneous monomer or CM concentration profile $\rho(z)$ (where z is the altitude) and extracting the osmotic pressure P from the measured

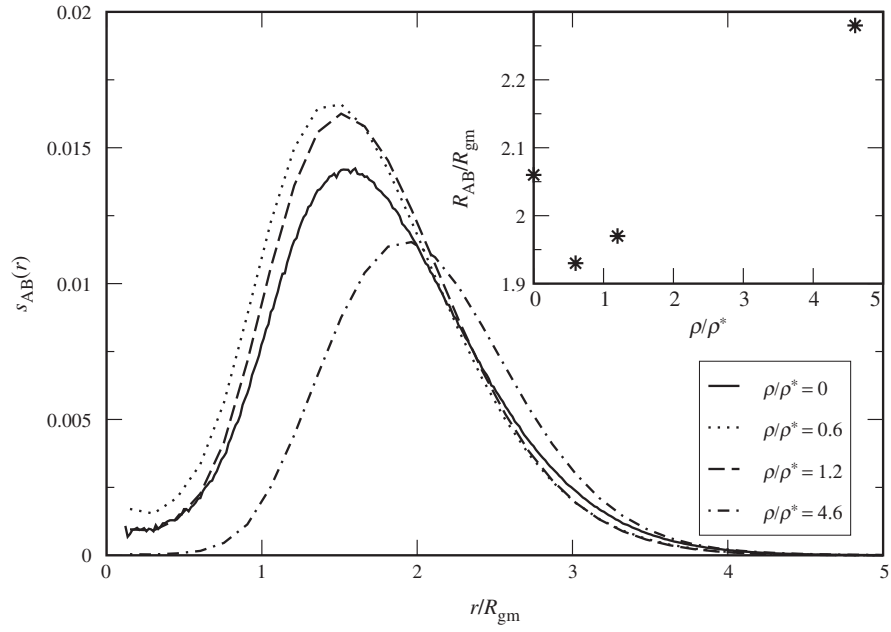

Figure 2. Intramolecular *CM* pair distribution function $s_{AB}(r)$ of the ISI model as a function of r/R_{gA} at four densities ρ/ρ^*. The inset shows R_{AB} (defined in equation (5)) versus ρ/ρ^*.

profile by invoking hydrostatic equilibrium [20, 21]

$$\frac{dP(z)}{dz} = -mg\rho(z), \tag{6}$$

where m is a fictitious buoyant mass and g is the acceleration due to gravity; these parameters may be adjusted in the simulation, such that the resulting sedimentation length $\zeta = k_B T/mg$ is larger than the polymer radius of gyration R_g, thus ensuring the validity of the macroscopic equation (6) on the mesoscopic scale set by R_g. A snapshot of a typical configuration in the sedimentation column is shown in figure 3, while the concentration profile $\rho(z)$ averaged over millions of such configurations generated in the MC run is plotted adjacent in the figure. The configuration in figure 3 clearly hints at the existence of microphase separation of the ISI model for copolymer concentrations $\rho/\rho^* \geq 2$. Horizontal cuts through the sedimentation column, shown in figure 4, exhibit alternating stripes of A and B strands, characteristic of the lamellar phase observed in many symmetric block copolymer melts [13, 14]. However, while the control parameter in melts is the temperature, the control parameter for the athermal ISI model is the polymer concentration.

Further evidence for the microphase separation comes from the osmotic equation of state, extracted from the concentration profile as explained above. The dimensionless equation of state $Z = P/\rho k_B T$, computed for copolymers with total number of monomers $2M$=120, 250, 500 and 2000, are plotted versus ρ/ρ^* in figure 5; no significant size dependence of Z is seen. Z increases from its infinite dilution limit 1 up to $\rho/\rho^* \approx 2.5$, where it reaches a maximum, before decreasing slowly to what appears to be an asymptotic value for $\rho/\rho^* > 10$. With increasing density the system moves from a disordered region to one where the lamellar order increases, and there are fewer interactions between A and B strands. The excess pressure (compared to ideal polymers) decreases in this region, as a consequence of the lamellar ordering which minimizes the number of A–B overlaps. The initial slope of $Z(\rho)$ agrees well with the second virial coefficient reported in table 1, while at high concentrations, the osmotic pressure increases sub-linearly with ρ/ρ^*. In future work the anisotropic pair structure will be calculated to characterize the onset of microphase separation in more detail.

4. Solving the inverse problem

We now return to the main objective of the present paper, namely to determine the effective pair potentials $v_{AA}(r)$, $v_{AB}(r)$ and $v_{BB}(r)$ between the *CM*s of A and B strands on different copolymers. In the case of the symmetric ISI model, $v_{AA}(r) = v_{BB}(r)$. From earlier work on homopolymers [5], which have coarse-grained interaction characterized by a single effective pair potential, we expect the effective pair potentials to be state dependent, i.e. to depend on polymer concentration. The subsequent discussion will be restricted to the

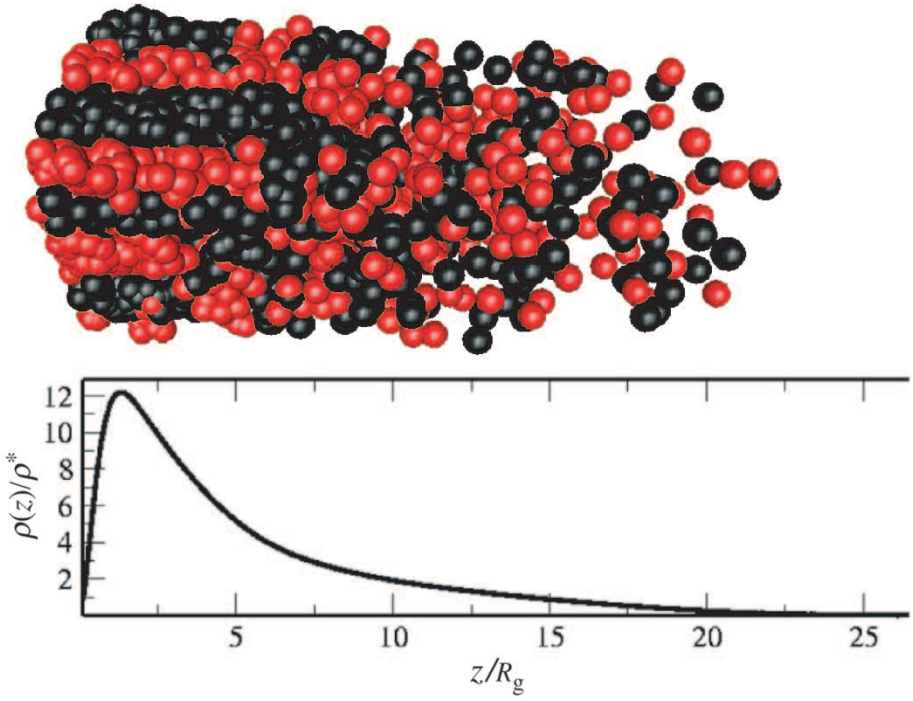

Figure 3. Top: typical configuration of $N = 1600$ ISI copolymers under gravity ($\zeta = k_B T/mg = 1.66R_g$). The copolymers are confined to a vertical box, open-ended in the z direction ($z > 0$), and periodically repeated in the horizontal x and y directions, the horizontal base is 100×100 lattice units. A and B strands are pictured as black and grey spheres of radius $R = R_{gA}$. Microphase separation into a striped pattern in clearly visible at lower altitudes. Bottom: monomer density profile $\rho(z)$ for the same system.

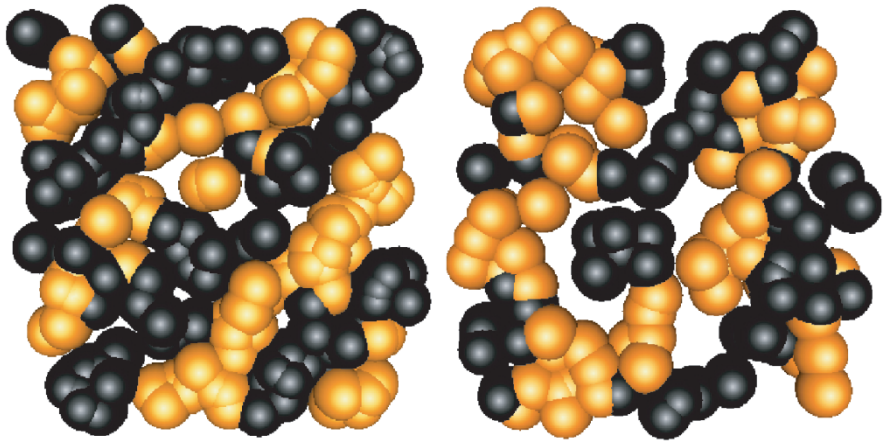

Figure 4. Two horizontal cuts of width $\Delta z = R_{gA}$ of the configuration in figure 3, at altitudes $z = 5.5R_g$ (left) and $z = 9.5R_g$ (right). A and B strands are again pictured as black and grey spheres of radius R_g. The lamellar structure is starting to break up at $z = 9.5R_g$.

limit of vanishing concentration, i.e. to an isolated pair of copolymers. To this end the intermolecular pair distribution functions $g_{AA}(r) = g_{BB}(r)$ and $g_{AB}(r)$ have been computed by MC simulations of a pair of AB copolymers. The procedure is similar to that used previously for homopolymers [5, 6], whereby conformations of the two isolated polymer coils are generated, and the *CM*s of the two coils are moved toward each other, while histograms are collected of the allowed configurations as a function of the *CM–CM* distance. In the case of diblock copolymers, care must be taken to correctly generate the partial $g_{\alpha\beta}(r)$. The simulation must be adjusted to move polymers such that the relevant CM_α–CM_β distance is changed. The MC results for the three low density pair distribution functions of the ISI model are shown in figure 6 together with

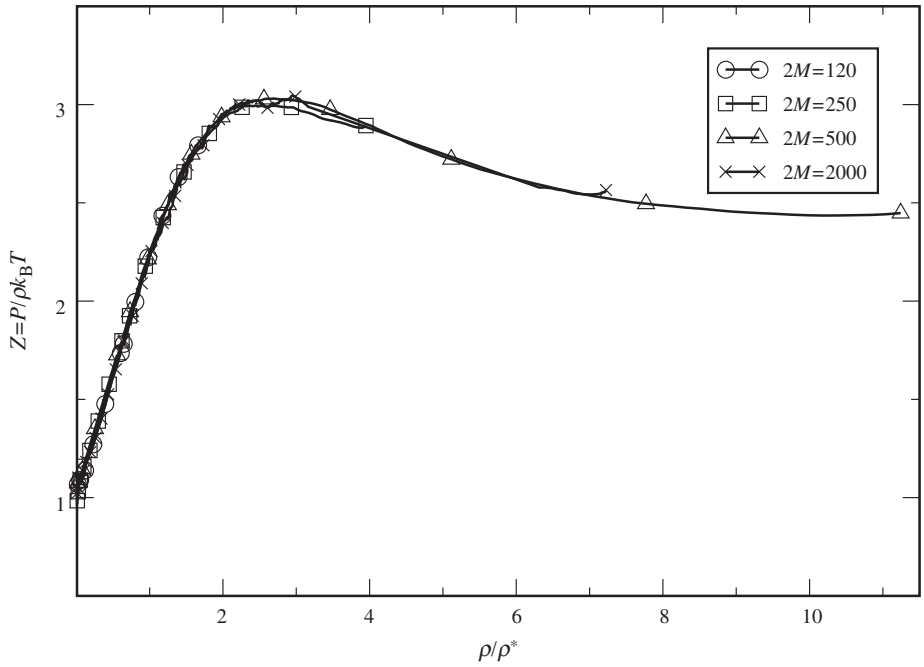

Figure 5. Osmotic equation of state $Z = P/(\rho k_B T)$ of the ISI model as a function of ρ/ρ^* as extracted from equation (6). The results are for copolymers of different lengths $2M = 120$, 250, 500 and 2000.

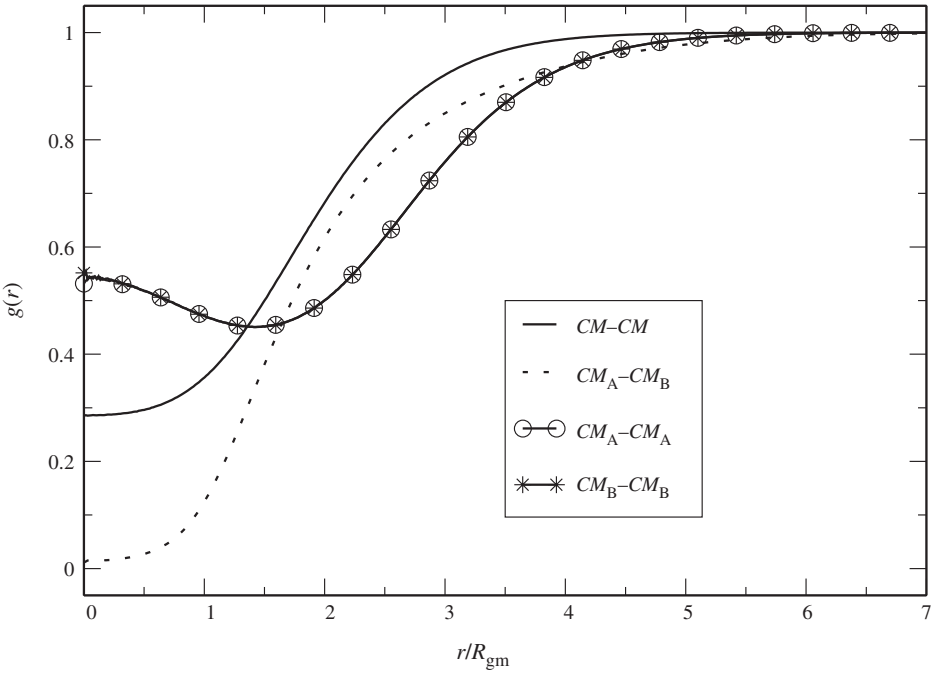

Figure 6. Zero density limit of the *CM* pair distribution functions $g_{AA}(r)$, $g_{AB}(r)$, $g_{BB}(r)$ and $g_{CC}(r)$ versus r/R_g. The results are from MC simulations of $2M = 500$ copolymers.

the pair distribution functions of the overall *CM*s of the copolymers, $g_{CC}(r)$. These results, together with the previously determined intramolecular pair distribution function $s_{AB}(r)$, are then inverted to yield effective, monomer-averaged pair potentials $v_{AA}(r) = v_{BB}(r)$, $v_{AB}(r)$ and $v_{CC}(r)$. While the inversion of $g_{CC}(r)$ to yield $v_{CC}(r)$ is trivial;

$$v_{CC}(r) = -k_B T \ln g_{CC}(r) \tag{7}$$

the inversion of $g_{AA}(r)$ and $g_{AB}(r)$ to yield $v_{AA}(r)$, $v_{AB}(r)$, given $s_{AB}(r)$ is considerably more complicated, since one is in effect facing a four-body problem. For site–site interaction models of 'diatomics', the exact relation between $g_{\alpha\beta}(r)$ and $v_{\alpha\beta}(r)$, for a given $s_{AB}(r)$, is in the low density limit [22]:

$$\begin{aligned}
&\lim_{\rho\to 0} h_{AA}(\mathbf{r}) \\
&= f_{AA}(\mathbf{r}) + [1 + f_{AA}(\mathbf{r})] \\
&\quad \times \left\{ \int d\mathbf{x}[f_{AB}(\mathbf{x})\, s_{BA}(\mathbf{x}-\mathbf{r}) + s_{AB}(\mathbf{x}) f_{BA}(\mathbf{x}-\mathbf{r})] \right. \\
&\qquad + \int d\mathbf{x} \int d\mathbf{y} s_{AB}(\mathbf{x})\, s_{BA}(\mathbf{y}-\mathbf{r})\,[f_{BB}(\mathbf{x}-\mathbf{y}) \\
&\qquad + f_{AB}(\mathbf{y}) f_{BB}(\mathbf{x}-\mathbf{y}) + f_{BA}(\mathbf{x}-\mathbf{r}) f_{BB}(\mathbf{x}-\mathbf{y}) \\
&\qquad + f_{AB}(\mathbf{y}) f_{BA}(\mathbf{x}-\mathbf{r}) \\
&\qquad \left. + f_{AB}(\mathbf{y}) f_{BA}(\mathbf{x}-\mathbf{r}) f_{BB}(\mathbf{x}-\mathbf{y})] \right\},
\end{aligned} \tag{8}$$

$$\begin{aligned}
&\lim_{\rho\to 0} h_{AB}(\mathbf{r}) \\
&= f_{AB}(\mathbf{r}) + [1 + f_{AB}(\mathbf{r})] \\
&\quad \times \left\{ \int d\mathbf{x}[f_{AA}(\mathbf{x})\, s_{AB}(\mathbf{x}-\mathbf{r}) + s_{AB}(\mathbf{x}) f_{BB}(\mathbf{x}-\mathbf{r})] \right. \\
&\qquad + \int d\mathbf{x} \int d\mathbf{y}\, s_{AB}(\mathbf{x})\, s_{AB}(\mathbf{y}-\mathbf{r})\,[f_{BA}(\mathbf{x}-\mathbf{y}) \\
&\qquad + f_{AA}(\mathbf{y}) f_{BA}(\mathbf{x}-\mathbf{y}) + f_{BB}(\mathbf{x}-\mathbf{r}) f_{BA}(\mathbf{x}-\mathbf{y}) \\
&\qquad \left. + f_{AA}(\mathbf{y}) f_{BB}(\mathbf{x}-\mathbf{r}) + f_{AA}(\mathbf{y}) f_{BB}(\mathbf{x}-\mathbf{r}) f_{BA}(\mathbf{x}-\mathbf{y})] \right\}.
\end{aligned} \tag{9}$$

where $h_{\alpha\beta}(\mathbf{r}) = g_{\alpha\beta}(\mathbf{r}) - 1$ and the $f_{\alpha\beta}(\mathbf{r})$ are the Mayer functions

$$f_{\alpha\beta}(\mathbf{r}) = f_{\beta\alpha}(\mathbf{r}) = \exp\left[-\beta v_{\alpha\beta}(\mathbf{r})\right] - 1. \tag{10}$$

The inversion procedure now amounts to solving the coupled integral equations (8) and (9) for the $f_{\alpha\beta}(r)$, using the $h_{\alpha\beta}(r)$ and $s_{\alpha\beta}(r)$ from the MC simulations as input. Once the $f_{\alpha\beta}(r)$ have been calculated by an appropriate iterative solution of the two coupled integral equations, the effective intermolecular potentials $v_{\alpha\beta}(r)$ follow from equation (10). The numerical solution of equations (8) and (9) is facilitated by the fact that all integrals on the right-hand side are convolution integrals, and hence easily evaluated by Fourier transformation, except the last term of the double integrals, which involves five factors and corresponds to a fully connected 'bridge' diagram, which cannot be resolved by Fourier transformation. If the bridge term is left out, in the spirit of the familiar hyper-netted chain (HNC) approximation [10], major difficulties are encountered when attempting a numerical solution, because of the inconsistency introduced by neglecting the bridge term, which is a violation of the connectivity constraints. However the task of including the bridge term may be achieved by noting that all integrals in equations (8) and (9) may be calculated analytically, if $s_{AB}(r)$, $f_{AA}(r)$, $f_{AB}(r)$ are sums of Gaussian functions centred on $r = 0$. We have hence fitted the MC data for $s_{AB}(r)$, shown in figure 2, by a sum of four Gaussian functions. The (two) unknown Mayer functions $f_{AA}(r) = f_{BB}(r)$, $f_{AB}(r)$ are represented by a sum of 10 Gaussian functions, and the amplitudes and widths are varied until the resulting pair correlation functions $4\pi r^2 h_{\alpha\beta}(r)$ yield the best fits to the MC data as illustrated in figure 7. The corresponding optimal Mayer functions $f_{AA}(r)$, $f_{AB}(r)$ and the resulting effective pair potentials $v_{AA}(r)$ and $v_{AB}(r)$ are plotted in figure 8. As expected, $v_{AA}(r) = v_{BB}(r)$ is small compared to $k_B T$ for all site–site distances, while $v_{AB}(r)$ is roughly Gaussian in shape, with an overlap ($v_{AB}(r = 0)$) value of $3.2 k_B T$. The effective pair potential $v_{CC}(r)$ between the overall copolymer *CM*s, calculated from equation (7) and the MC data for $g_{CC}(r)$, is also shown in figure 8. Its amplitude at full overlap, $v_{CC}(r = 0) \approx 1.25 k_B T$ is almost three times smaller than $v_{AB}(r = 0)$ but its range is significantly wider, as one may expect, since the effective potential $v_{CC}(r)$ involves an implicit averaging over relative orientations of the elongated diblock copolymers. It is interesting to note that the entropic barrier of $3.2 k_B T$ for complete overlap of the mutually avoiding strands A and B of the two copolymers is substantially higher than found for homopolymers, where $v(r = 0) \approx 1.8 k_B T$ for sufficiently long polymers [4, 5, 9]. This is a consequence of the fact that monomers of the same strand can overlap (ideal polymers), and that the strands are hence more compact than the swollen self-avoiding walk polymers. Interestingly, the effective potential $v_{AB}(r)$ for two copolymers is rather close to that found for binary mixtures of untethered A and B polymers [23].

5. Conclusion

We have introduced and investigated a highly simplified model of a symmetric diblock copolymer which leads to microphase separation, the ISI model. The binary mixture counterpart of ISI, where A and B strands are

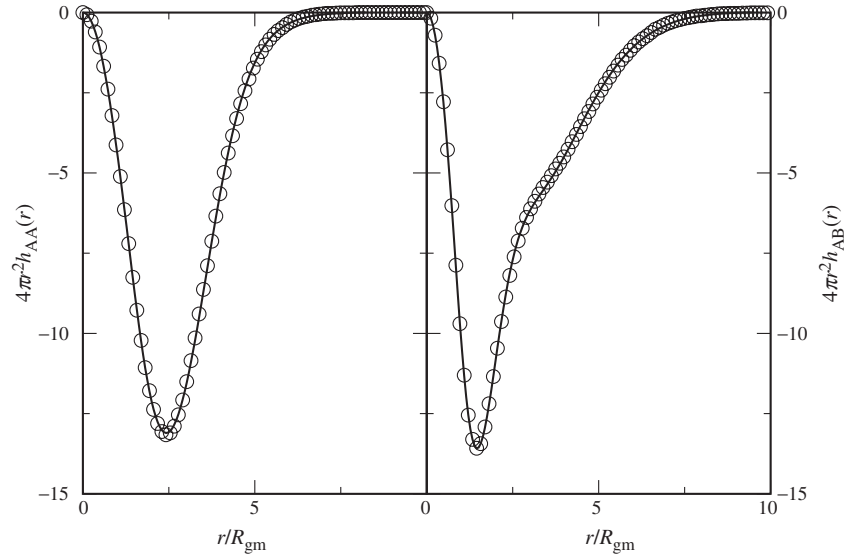

Figure 7. Optimal representation of the MC data for $4\pi r^2 h_{AA}(r)$ and $4\pi r^2 h_{AB}(r)$ of the ISI model in the zero density limit, achieved by the inversion procedure of equations (8), (9) and (10). The unknown $f_{\alpha\beta}(r)$ are parametrized by sums of 10 Gaussian functions.

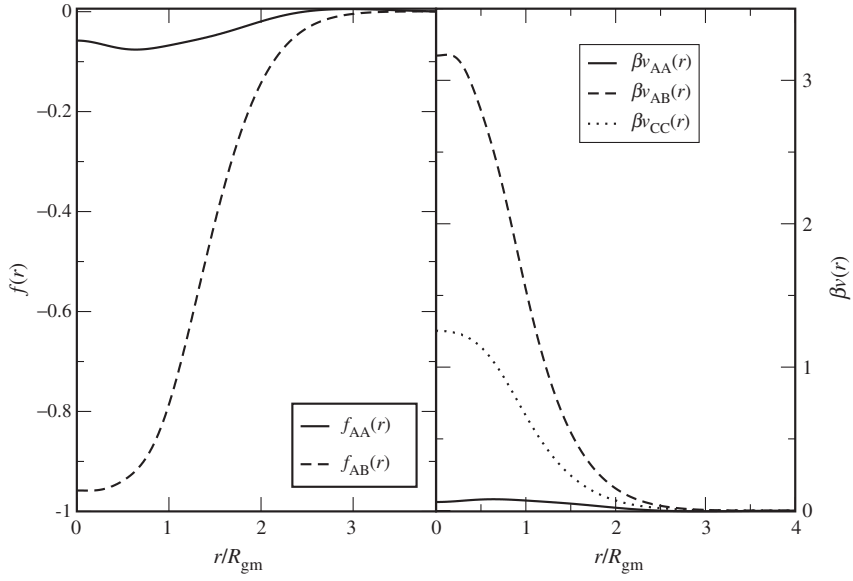

Figure 8. Left: Mayer functions $f_{AA}(r) = f_{BB}(r)$ and $f_{AB}(r)$ versus r/R_{gm}, as derived by the inversion procedure outlined in the text and in figure 7. Right: resulting effective pair potentials, $v_{AA}(r) = v_{BB}(r)$, $v_{AB}(r)$ and $v_{CC}(r)$, versus r/R_{gm}; the effective potentials correspond to the zero density limit.

untethered is the macromolecular equivalent of the Widom–Rowlinson model [12], and like the latter leads to macroscopic phase separation [23]. Despite the simplicity of the ISI model, a fully quantitative investigation of its structure, thermodynamics and phase behaviour would still be a daunting task, and only partial results have been reported in the present paper. In order to go further we propose a coarse-graining strategy, whereby an AB block copolymer is schematized by two 'blobs' tethered by an entropic spring, deriving from an effective intramolecular pair potential $\phi_{AB}(r)$ between the *CM*s of the two strands. We were able to extract $\phi_{AB}(r)$ and the intermolecular potentials $v_{AA}(r)$ and $v_{AB}(r)$ from the site–site pair distribution functions $s_{AB}(r)$, $g_{AA}(r)$, $g_{AB}(r)$ in the zero density limit, as generated by MC simulations for an isolated pair of interacting copolymers with $2M$ monomers ($10^2 \lesssim M \lesssim 10^3$). The simulation of the resulting coarse-grained 'soft diatomic'

representation of the ISI model is orders of magnitude faster, since the number of degrees of freedom is reduced by a factor M. Preliminary investigations show that the coarse-grained model indeed leads to phase behaviour very similar to that of the original ISI model. Note that, by construction, the 'soft diatomic' model will lead back to the exact pair distribution functions of the ISI, at least at zero density. From our earlier experience with effective pair potentials between the *CM*s of homopolymers, we expect some concentration dependence of the effective potentials for AB copolymers. In the case of the former, the inversion of the single pair distribution function at finite polymer concentration is straightforward, via the HNC closure which is extremely accurate for soft potentials [5, 6]. A similar inversion scheme for diblock copolymers could in principle be based on the 'reference interaction site model' (RISM) formalism [24], with HNC closure, but the inconsistencies of this formalism are well documented, and will require careful attention for its implementation in an inversion procedure. Since no dramatic density dependence of the effective potentials is expected, at least for the athermal ISI model, an excellent first approximation will be to use the zero density potentials derived in the present paper to investigate the behaviour of dilute and semi-dilute copolymer solutions. A severe check will be provided by a direct comparison of the pair distribution functions obtained at finite densities with the effective 'soft diatomic' model, and from the full underlying ISI model. Work along these lines is in progress. The extension of the present work to asymmetric ($M_A \neq M_B$) diblock, triblock and more complex copolymer systems is, at least in principle, straightforward.

Acknowledgements

C. Addison wishes to thank the EPSRC for a studentship, and A. Louis is grateful to the Royal Society for a university research fellowship. The authors found constant inspiration in the ideas and papers of Ben Widom.

References

[1] C.N. Likos. *Phys. Rep.*, **348**, 267 (2001).
[2] A.A. Louis. *Phil. Trans. R. Soc. Ser.* A, **359**, 939 (2001).
[3] J.-P. Hansen, H. Löwen. In *Bridging Time Scales: Molecular Simulations for the Next Decade*, P. Nielaba, M. Mareschal, G. Ciccotti (Eds), pp. 167–196, Springer Verlag, Berlin (2002).
[4] J. Dautenhahn, C.K. Hall. *Macromolecules*, **27**, 5399 (1994).
[5] P.G. Bolhuis, A.A. Louis, J.-P. Hansen, E.J. Meijer. *J. chem. Phys.*, **114**, 4296 (2001).
[6] V. Krakoviack, J.-P. Hansen, A.A. Louis. *Phys. Rev.* E, **67**, 041801 (2003).
[7] G. Yatsenko, E.J. Sambriski, M.A. Nemirovskaya, M. Guenza. *PRL*, **93**, 257803 (2004).
[8] C.N. Likos, H. Löwen, M. Watzlawek, B. Abbas, O. Jucknischke, J. Allgaier, D. Richter. *Phys. Rev. Lett.*, **80**, 4450 (1998).
[9] A. Pelissetto, J.-P. Hansen. *J. chem. Phys.*, **122**, 134904 (2005).
[10] J.-P. Hansen, I.R. McDonald, *Theory of Simple Liquids*, 2nd edn., Academic Press, London (1986).
[11] J.S. Rowlinson, B. Widom, *Molecular Theory of Capillarity*, Clarendon Press, Oxford (1982).
[12] B. Widom, J.S. Rowlinson. *J. chem. Phys.*, **52**, 1670 (1970).
[13] F.S. Bates, G.H. Frederickson. *Annu. Rev. Phys. chem.*, **41**, 525 (1990).
[14] K. Binder. *Adv. Polym. Sci.*, **112**, 181 (1994).
[15] For a recent discussion, see C.I. Addison, A.A. Louis, J.P. Hansen. *J. chem. Phys.*, **121**, 612 (2004).
[16] O.F. Olaj, B. Neubauer, G. Zifferer. *Macromol. Theo. Simul.*, **7**, 171 (1998).
[17] M. Lal. *Molec. Phys.*, **17**, 57 (1969).
[18] N. Madras, A.D. Sokal. *J. stat. Phys.*, **50**, 109 (1988).
[19] See e.g. B. Li, N. Madras, A.D. Sokal. *J. stat. Phys.*, **80**, 61 (1995).
[20] C.I. Addison, A.A. Louis, J.-P. Hansen. to be published (2005).
[21] T. Biben, J.-P. Hansen, J.L. Barrat. *J. chem. Phys.*, **98**, 7330 (1993).
[22] B.M. Ladanyi, D. Chandler. *J. chem. Phys.*, **62**, 4308 (1975).
[23] C.I. Addison, P.A. Artola, J.-P. Hansen, A.A. Louis. to be published (2005).
[24] For a review, see D. Chandler. In *Studies in Statistical Mechanics*, J.L. Lebowitz, E.W. Montroll (Eds), Vol. 8, p. 275, North Holland, Amsterdam (1982).